Redox Biology 18 (2018) 43–53

Contents lists available at ScienceDirect

Redox Biology

journal homepage: www.elsevier.com/locate/redox

Effects of the stimuli-dependent enrichment of 8-oxoguanine DNA glycosylase1 on chromatinized DNA

Wenjing Hao[a,1,2], Tianyang Qi[a,2,3], Lang Pan[a,3,4], Ruoxi Wang[a,b,c,1], Bing Zhu[a], Leopoldo Aguilera-Aguirre[a], Zsolt Radak[a,5], Tapas K. Hazra[b,c], Spiros A. Vlahopoulos[a,6], Attila Bacsi[a,7], Allan R. Brasier[b,c], Xueqing Ba[a,1], Istvan Boldogh[a,c,*]

[a] Department of Microbiology and Immunology, University of Texas Medical Branch at Galveston, Galveston, TX 77555, USA
[b] Internal Medicine, University of Texas Medical Branch at Galveston, Galveston, TX 77555, USA
[c] Sealy Center for Molecular Medicine, University of Texas Medical Branch at Galveston, Galveston, TX 77555, USA

ARTICLE INFO

Keywords:
Oxidative DNA damage
8-oxoguanine
Epigenetic
Gene expression

ABSTRACT

8-Oxoguanine DNA glycosylase 1 (OGG1) initiates the base excision repair pathway by removing one of the most abundant DNA lesions, 8-oxo-7,8-dihydroguanine (8-oxoG). Recent data showed that 8-oxoG not only is a pro-mutagenic genomic base lesion, but also functions as an epigenetic mark and that consequently OGG1 acquire distinct roles in modulation of gene expression. In support, lack of functional OGG1 in *Ogg1*$^{-/-}$ mice led to an altered expression of genes including those responsible for the aberrant innate and adaptive immune responses and susceptibility to metabolic disorders. Therefore, the present study examined stimulus-driven OGG1-DNA interactions at whole genome level using chromatin immunoprecipitation (ChIP)-coupled sequencing, and the roles of OGG1 enriched on the genome were validated by molecular and system-level approaches. Results showed that signaling levels of cellular ROS generated by TNFα, induced enrichment of OGG1 at specific sites of chromatinized DNA, primarily in the regulatory regions of genes. OGG1-ChIP-ed genes are associated with important cellular and biological processes and OGG1 enrichment was limited to a time scale required for immediate cellular responses. Prevention of OGG1-DNA interactions by siRNA depletion led to modulation of NF-κB's DNA occupancy and differential expression of genes. Taken together these data show TNFα-ROS-driven enrichment of OGG1 at gene regulatory regions in the chromatinized DNA, which is a prerequisite to modulation of gene expression for prompt cellular responses to oxidant stress.

1. Introduction

Oxidatively modified DNA base and strand lesions are genotoxic, mutagenic, and implicated in various human pathologies [1,2]. While their levels in DNA vary according to sequence context, chromatin accessibility, and the nature of the oxidants, 7, 8-dihydro-8-oxoguanine (8-oxoG) is the most abundant lesion due to guanine (G) having the lowest redox potential among the four nucleobases [3,4]. Although 8-oxoG and other oxidatively modified G lesions (2,6-diamino-4-hydroxy-5-formamidopyrimidine: FapyG, spiro-, and guano-hydantoins) can be

Abbreviations: 8-oxoG, 8-oxo-7, 8-dihydroguanine; AP, apurinic/apyrimidinic site in DNA; APE1, apurinic/apyrimidinic endonuclease 1; BER, base excision repair; ChIP, chromatin immunoprecipitation assays; ChIP-seq, chromatin immunoprecipitation assays followed by DNA sequencing; CXCL-1, CXC-motif chemokine ligand-1 (protein); *CXCL*, human gene or mRNA encoding CXCL-1; CCL, CC chemokine ligand; CCL, gene or mRNA encoding CC chemokine ligand; GEO, Gene Expression Omnibus; GO, gene ontology; GOrilla, Gene Ontology enRIchment anaLysis and visuaLizAtion tool; IIR, innate immune response;; OGG1, 8-oxoguanine DNA glycosylase-1 protein; OGG1-BER, OGG1-initiated DNA base excision repair; ROS, reactive oxygen species; NF-κB, Nuclear Factor kappa B; RNA Pol II, RNA polymerase II; Sp1, specificity protein 1; TFIID, transcription initiation factor II-D; TNFα, tumor necrosis factor alpha; TSS, transcription start site

* Correspondence to: Department of Microbiology and Immunology University of Texas Medical Branch at Galveston, 301 University Blvd, Galveston, TX 77555-1070, USA.
E-mail address: sboldogh@utmb.edu (I. Boldogh).
[1] School of Life Science, Northeast Normal University, Changchun, China.
[2] Wenjing Hao and Tianyang Qi contributed equally to this work.
[3] Science Research Center of China-Japan Union Hospital, Jilin University, Changchun, China.
[4] Department of Physiology, Xiangya Medicine School in Central South University, Changsha, Hunan 410078, China.
[5] Research Institute of Sport Science, Semmelweis University, Budapest, Hungary.
[6] National and Kapodistrian University of Athens, Faculty of Medicine, Athens, Greece.
[7] Department of Immunology, Faculty of Medicine, University of Debrecen, Hungary.

https://doi.org/10.1016/j.redox.2018.06.002
Received 27 April 2018; Received in revised form 4 June 2018; Accepted 6 June 2018
Available online 12 June 2018

repaired by base-specific DNA repair enzymes, including Nei-like 1 and 2 (NEIL1, NEIL2) glycosylases [5–7], OGG1 is the primary glycosylase to remove 8-oxoG. OGG1 has base excision and associated AP lyase activities. The latter cleaves DNA at abasic site via a β-elimination mechanism and generates a 3′-phospho-α, β-unsaturated aldehyde terminus (3'dRP) and 5'-phosphate (apurinic/apyrimidinic [AP]) site. AP sites are removed by apurinic/apyrimidinic endonuclease 1 (APE1) to form polymerase-ready 3'OH residues. Gap filling can involve 1-nt incorporation by DNA polymerase β (Polβ) in the short-patch repair sub-pathway or the displacement synthesis of 2–8 nts by either Polβ or replicative DNA polymerase delta in the long-patch repair sub-pathway [5,8,9].

Guanine oxidation is linked to mutagenesis and many pathologies; however, *Ogg1* knock out (*Ogg1*$^{-/-}$) mice are viable, have unaltered lifespan, display no marked pathological changes, and show moderate mutation rate despite supra-physiological levels of 8-oxoG in their genomes [10–12]. In spite of the well-defined roles of OGG1 in removal of oxidative DNA base lesion(s), the decreased immune responses to various inflammatory agents including TNFα, lypopolysacharide, allergens, or *Helicobacter pylori* infection [13–15] as well as development of metabolic disorders in *Ogg1*$^{-/-}$ mice [16,17] indicate additional functions of OGG1.

Recent studies showed that 8-oxoG may function as an epigenetic mark and OGG1 has distinct roles in regulation of gene expression (for reviews see [18–20]). For example, increased formation of 8-oxoG in guanine-rich proximal promoter regions of hypoxia-modulated genes was accompanied by BER function of OGG1 followed by transcriptional activation [21–23]. Another study showed that OGG1 (via its AP lyase activity) introduces a nick into the DNA strand and provides an entry point for topoisomerase II-β promoting estrogen-induced gene expression [24]. In this experimental system, guanine oxidations were initiated onsite by histone demethylation via DNA lysine demethylase1 (LSD1) [24,25]. Similar LSD1-dependent guanine oxidation, OGG1 recruitment, and transcriptional activation of genes were observed in retinoic acid and androgens challenged cells [26,27]. A study by Seifermann and co-workers demonstrated the existence of an OGG1 and LSD1 dependent mechanism of *TNF* expression upon activation of macrophages by LPS [28]. Dr. Burrows and colleagues demonstrated that 8-oxoG in potential G-quadruplex-forming sequences in the promoter is a signaling entity and that only OGG1's enzymatic activity is needed for the initiation of gene expression [29–31].

Studies have also shown that cytokine exposure of cells increased 8-oxoG levels primarily in gene regulatory sequences along with enzymatic inactivation of OGG1 [32,33]. Oxidatively inactivated OGG1 recognizes and binds genomic 8-oxoG without its excision, which was linked to the prompt expression of chemokines and cytokines and consequent inflammatory response [19,33,34]. Our studies using chromatin immunoprecipitation, also revealed that the OGG1-DNA interaction in promoter sequences of C-X-C motif chemokine ligand 2 (*Cxcl*2) facilitates the recruitment of the sequence-specific transacting factors nuclear factor kappaB (NF-κB) and specificity protein 1 (Sp1), general transcription factor II-D (TFIID), and phosphorylated RNA polymerase II (p-RNA pol II) [32]. Consistent with these data, OGG1 bound to DNA at 8-oxoG upstream from the NF-κB binding motif, increased its DNA occupancy by promoting the binding of both the homodimeric and heterodimeric forms of NF-κB [33,34].

Here, we performed chromatin immunoprecipitation-coupled sequencing (ChIP-seq) to examine the stimulus-driven association of OGG1 with chromatinized DNA. Our analysis revealed that ROS generated by TNFα exposure of cells led to OGG1 enrichment primarily at the regulatory regions of a large number of genes for an immediate global cellular response. OGG1 recruited to specific genomic regions is functional, and OGG1 antibody ChIP-ed genes are constitute various signal transduction pathways and are predicted to modulate complex biological processes involving metabolic and immune responses.

2. Materials and methods

2.1. Reagents and antibodies

TNFα was purchased from PeproTech Inc (Rocky Hill, NJ); Tris, NaCl, EDTA, EGTA, Nonidet P-40, sodium pyrophosphate, glycerophosphate, Na_3VO_4, NaF, aprotin/leupeptin/PMSF, sodium dodecyl sulfate, and paraformaldehyde were from MilliporeSigma (St Louis, MO, USA). Antibodies (Abs) to RelA(NF-κB) (Cat # sc-8008 ×; Santa Cruz Biotech; Santa Cruz, CA), control IgG (Cat # sc-2025; Santa Cruz Biotech). Anti-OGG1 and anti-Flag (M2, Cat # F1804) Abs were from Abcam (Cambridge, MA, USA) and MilliporeSigma, respectively.

2.2. Cell cultures

Human Embryonic Kidney 293 (HEK 293); ATCC; American Type Culture Collection) cells were maintained in MEM medium. The media was supplemented with 10% fetal bovine serum (Hyclone, GE, Healthcare Life Sci. LTD), penicillin (100 units/ml; GIBCO-BRL, Gaithesburg, MD, USA), and streptomycin (100 μg/ml; GIBCO-BRL). Cells were regularly tested for mycoplasma contamination.

2.3. siRNA-mediated depletion of gene expression

To deplete OGG1 expression from cultured cells, small interfering (si)RNA transfection was performed using Lipofectamine® RNAiMAX reagent (Thermo Fisher Scientific), per the manufacturer's instructions. siRNA to down-regulate human OGG1 (Cat# M-005147–03-0005) was purchased from Dharmacon (Pittsburg, PA, USA). Extent of OGG1 depletions were determined by real-time PCR and Western blotting [35].

2.4. Electrophoretic mobility shift assay (EMSA)

Nuclear extracts (NE) were prepared using a CelLytic™NuCLEAR™ Extraction Kit (NXTRACT, Sigma-Aldrich) and protein concentration was determined with the DC™ Protein Assay Kit (Bio-Rad). Biotinylated wild-type, 8-oxoG and NF-κB binding site-containing double-stranded oligonucleotide probes were used for EMSA. Probes (10 fmol) were mixed with NE (2 μg) for 10 min at room temperature in buffer containing 2 mM HEPES (pH 7.5), 4 mM KCl, 1 mM dithiothreitol (DTT), 0.25 mM $MgCl_2$, 0.001% NP-40, 50 ng/μl of poly(dI-dC) and 1 mg/ml BSA. Unlabeled probes were used for competition experiments. Samples were resolved on a 6% DNA retardation gel (Invitrogen) in 0.25 × Tris/Borate/EDTA (TBE) buffer. Visualization of NF-κB-DNA complexes was carried out with LightShift chemiluminescent EMSA kit (Thermo scientific) with modifications). Probes: Wild type (P^{WT}): 5'-TGGGGAGTG TGAGGGGTATCCGATGCTTG-3') and 8-oxoG containing (P^{*}): 5'-TG* GGGAGTGTGAGGGGTATCCGATGCTTG-3'; complementary strand was wild type: 5'-CAAGCATCGGATACCCCTCACACTCCCC-3' sequence. Underlined sequences show NF-κB motifs.

2.5. RNA extraction and real-time PCR analysis

Total RNAs were extracted using an RNeasy total RNA purification kit according to the manufacturer's instructions (Qiagen). Complementary DNA was synthesized from 1 μg of total RNA using an iScript cDNA synthesis kit with oligo (dT) and random primers (Bio-Rad Laboratories). Transcript levels of genes were quantitated by qPCR using iQ SYBR green supermix (Bio-Rad Laboratories) with gene-specific primers from Integrated DNA Technologies (see below). Gene expression values were calculated on the basis of the $2^{-\Delta\Delta CT}$ method and normalized with internal control, glyceraldehyde-3-phosphate dehydrogenase (GAPDH) [35]. Primers: h*GAPDH*, forward (F), 5'-TGTAGT TGAGGTCAATGAA GGG-3', reverse (R), 5'-ACATCGCTCAGACACC ATG-3'; *TNF*, F, 5'-TCAGCTTGAGGGTTTGCTAC-3', R, 5'-TGCACTTTG GAGTGATCGG-3'; *CXCL1*, F, 5'-TCTCTCTTTCCTCTTCTGTTCCTA − 3',

R, 5'-CATCCCCCATAGTTAAGAAAATCATC-3'; *CXCL2,* F, 5'-TGTTTGAGCATCACTTAGGAGAA-3', R, 5'- CCCTGCCGTCACATTGATCT-3'; *CXCL3, F,* 5'-TGCCCTTACCAGAGCTGAAA-3', *R,* TTGCTTGCATTTCAATCCCCC-3'*; CXCL8/IL8, F, 5-CCAGGAAGAAACCACCGGAA-5',* R, *5'-ATGAATTCTCAGCCCTCTTCAA-3';* h*OGG1*, F, 5'-CAGAAGATAAGAGGACGCAGAAG-3', R, 5'-CATATGAGGAGGCCCACAAG − 3'. Human Inflammatory Cytokines and Receptors Arrays (SABiosciences, PAHS-011Z) were used as recommended by manufacturer. Data were analyzed using RT2 profiler PCR data analysis template version 2.0. The results were reported as mean fold increases for all experimental groups, and data sets were deposited in the National Center for Biotechnology Information. Gene Expression Omnibus accession number is GSE75652 (http://www.ncbi.nlm.nih.gov/geo/query/acc.cgi?acc=GSE75652).

2.6. Chromatin Immunoprecipitation (ChIP) Assay

ChIP assays were performed as described previously [36] with slight modifications. Briefly, parallel cultures of HEK 293 cells were transfected with Flag-OGG1 expression vector and 30 h thereafter cells were stimulated with TNFα for 0, 15, 30 and 60 min. The cells were harvested, and ChIP assays performed using Abs against FLAG, RelA(NF-κB) or IgG. ChIP reagents were used according to the recommended protocol from Millipore Corporation (Billerica, MA, USA). Cells (5×10^6) were cross-linked with 1% paraformaldehyde and sheared with 10-second pulses using Cole-Parmer's GEX 130 Ultrasonic processor (Vernon Hills, IL, USA) equipped with 2-mm tip and set to 30% of maximum power. One ml of the 10-fold diluted reaction mixture was incubated with or without Abs and then immunoprecipitated (IP) with protein A- or G-agarose (Millipore, Corporation Billerica, MA, USA) blocked with salmon sperm DNA. Before adding Abs (Flag, RelA(NF-κB) and agarose beads, one tenth of the dilution was directly subjected to DNA extraction and used as input. The precipitates were washed extensively, de-cross-linked, and subjected to RT-PCR. Primers for PCR amplification are listed in Table 1. ChIP-qPCR calculations were performed as described previously [37]. In brief, protein specific Ab ChIP-ed DNA signal intensity value was divided by the intensity value of the IgG-ChIP-ed signal, representing the fold enrichment of the protein on the specific region of genomic DNA.

2.7. ChIP-sequencing and analysis

Immunoprecipitated DNA was isolated and DNA fragments (300 ± 25 bp) were gel purified. Approximately 10 ng of OGG1 and RelA(NF-κB) Ab- as well as IgG-ChIP-ed DNA was sequenced by high-throughput DNA sequencing using a Solexa/Illumina genome analyzer (Ambry Genetics). All sequence reads produced by the Illumina genome analyzer were analyzed by base calling and sequence quality filtering scripts using the Illumina Pipeline software (version 1.4.0; Illumina, Hayward, CA) at UTMB's Next-Generation Sequencing (NGS) Core Facility (Director: Dr. Thomas G. Wood). ChIP-Seq data have been deposited in the NCBI's Gene Expression Omnibus (GEO) and is accessible through the GEO Series accession number GSE89017. The raw data were submitted for analysis to BioInfoRx LESS™ (Lab Essential Software Solutions) (https://bioinforx.com/lims2/; Madison, WI). The sequence reads were analyzed by Model-based Analysis of ChIP-Seq (MACS) program [38]. ChIP-ed sequences were aligned to the reference human genome assembly GRCh38/hg38). BED and wiggle (WIG) files were created using the University of California at Santa Cruz (UCSC) Genome Browser (http://genome.ucsc.edu/index.html). To identify potential regulatory elements in OGG1 and NF-κB-ChIP-ed sequences, Hypergeometric Optimization of Motif EnRichment (HOMER) (http://homer.ucsd.edu/homer/ motif/index.html) was utilized. HOMER is a motif discovery algorithm (findMotifs.pl and findMotifsGenome.pl), that identifies motifs in promoter and genomic regions, respectively (https://bioinforx.com/lims2/). To obtain visual locations of enrichment peaks, the high-performance visualization tool, Integrative Genomics Viewer (IGV; http://software.broadinstitute.org/software/igv/home) was utilized [39,40].

Table 1
The sequence of PCR primers used in this study.

Gene name	Base pairs	Location	Sequence
TNFα	197	Promoter	F: 5'- CTTGTGTGTCCCCAACTT − 3' R: 5'- TCTTTGAGATCCATGCCGTTG − 3'
CXCL1	200	Promoter	F: 5'- GGAGTTACTCTGAAGGGCGAG − 3' R: 5'- AAAGGGGTTCGCGGATCTC − 3'
NFKBIB	232	Promoter-Exon1	F: 5'- GAGAGTTGTAGTCCTCCCGA − 3' R: 5'- GTCGGCAGCTTTTCCCAAG − 3'
RELA	276	Promoter	F: 5'- GCATCTAGATTGGGGTGGGT − 3' R: 5'- CCGCCGATTACTCACTTTGT − 3'
IL6	233	Promoter-Exon1	F: 5'- CTTGCCATGCTAAAGGACGT − 3' R: 5'- CCTGGAGGGGAGATAGAGCT − 3'
ICAM1	213	Promoter	F: 5'- TAACAGTCTCCACTCTCCGG − 3' R: 5'- GTCATCCTCCCTCGCTGG − 3'
CXCL12	117	Exon1	F: 5'- CGGAGCCTGAGAAGGTCA − 3' R: 5'- GGCTGACGGAGAGTGAAAG − 3'
CXCL5	127	Promoter-Exon1	F: 5'- CCACCAGTTCCCATTGTCTG − 3' R: 5'- TCTACACTCATCTCTCCCCAC − 3'
NGF	214	Promoter	F: 5'- GCGGAGAGGTGAGGGAAG − 3' R: 5'- GGGGACTACAGACGGATCG − 3'
CXCL6	268	Promoter-Exon1	F: 5'- TCGCTGCTCTATTTTGGCTG − 3' R: 5'- AGCACTTTGGTTTCCTCGTG − 3'
LTA	241	Exon1	F: 5'- GTGGTTCTCTCCTAGGCCTC − 3' R: 5'- CGGTAGTCCAAAGCACGAAG − 3'
CCL20	298	Promoter	F: 5'- GGAATGTTCCTGTGTGGGG − 3' R: 5'- TTGCCACATGGGGTTTTCC − 3'

2.8. Gene ontology and gene interaction analysis

Gene ontology (GO) and signaling pathways were analyzed by Gene Ontology enRIchment anaLysis and visuaLizAtion tool (GOrilla; http://cbl-gorilla.cs.technion.ac.il/. GOrilla employs flexible threshold statistical approaches to discover GO terms that are significantly enriched at the top of a ranked gene list. GOrilla computes an exact p-value for the observed enrichment, taking threshold multiple testing into account without the need for simulations [41]. The output of the enrichment analysis is visualized as a hierarchical structure, providing a clear view of the relations between enriched GO terms.

To identify gene sets involved in specific biological processes, the GeneCards database integrated from the Human Genome Organization, Gene Nomenclature Committee, European Bioinformatics Institute, and National Center for Biotechnology Information and Database of Allergy and Asthma Biomarkers, and others, were utilized (http://www.genecards.org).

2.9. Statistical analysis

Statistical analyses were performed using Student's *t*-test to analyze changes at the mRNA and protein levels. Data from treatment groups were analyzed by using ANOVA, followed by Bonferroni post-hoc analyses for least significant difference. The data presented as the means ± the standard error of the mean. Differences were considered to be statistically significant at $p < 0.05$.

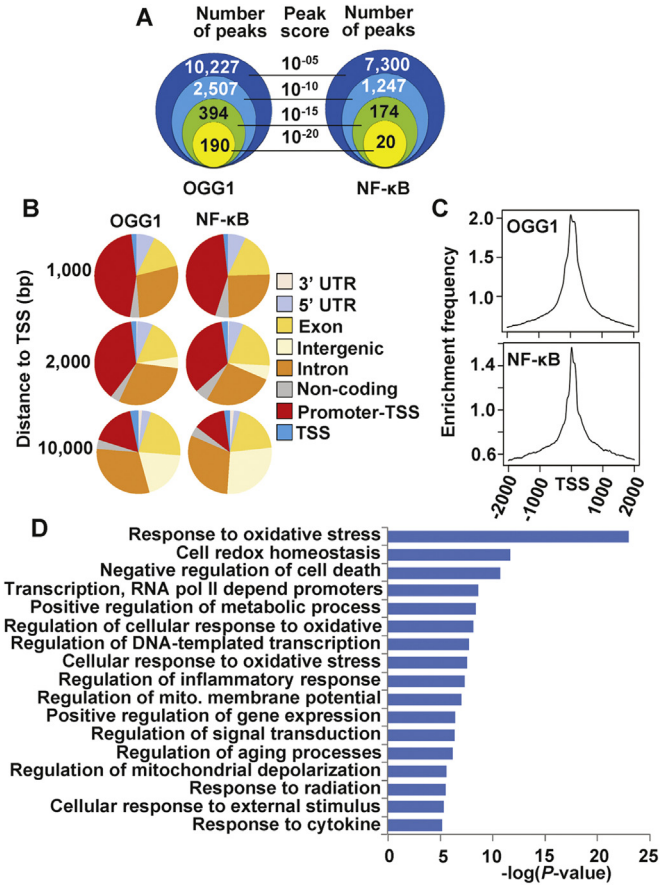

Fig. 1. Stimulus-induced enrichment of OGG1 on gene regulatory regions at the level of whole-genome and overrepresented biological processes associated with OGG1 Ab-ChIP-ed genes. A, Graphical depiction of peak numbers for OGG1. As control, numbers of enrichment peaks for NF-κB are shown. B, Distribution of OGG1 and NF-κB enrichment peaks as a function of distance from TSS (± 1000 bp, upper panel; ± 2000 bp, middle panel and ± 10,000 bp, lower panel). C, Histogram of the OGG1 and NF-κB distribution on TSS-adjacent sequences ± 2000 bp at the whole-genome level. D, Overrepresented biological processes associated with OGG1 ChIP-ed genes. A ranked list of OGG1 ChIP-ed (peak score from $< 10^{-5}$ to $< 10^{-20}$) genes was submitted to the Gene Ontology enRIchment anaLysis and visuaLizAtion tool (GOrilla). The overrepresentation levels of each biological process are expressed as –log (*P* value) and calculated using Microsoft Excel. B, C, Lists of TSSs were generated by the human TSS track (Switchgear Genomics via the USCS Genome Browser [51]). Reports of the distances from the best TSS are plotted. Data for the 30 min time point are shown. TSS, transcription start site.

3. Results

3.1. ROS generated by TNFα induced enrichment of OGG1 in the chromatinized DNA

FLAG-OGG1 (OGG1)-expressing cells were exposed to a physiologically relevant dose of ROS generated by TNFα (TNFα-ROS) [32,42]. At times 0, 15, 30, and 60 min, DNAs were ChIP-ed using antibodies (Abs) to OGG1 (anti-FLAG Ab), or IgG. Both ROS- and TNFα are activators of NF-κB of which sequence-specific binding in the chromatin is well characterized [43–45], therefore ChIP with RelA(NF-κB) Ab served as a control. The replicates of ChIP-ed DNA samples were sequenced and reads were aligned and mapped to the human genome (hg38). Enrichment peaks that were 4-fold over the background and shown to have a cumulative Poisson *P*-value of less than 0.0001 were taken into account. The sequence alignment analysis showed that the OGG1 enrichment occurred at specific genomic regions from 15 min onward and reached the maximum at 30 min after TNFα exposure. The enrichment peaks were primarily associated with guanine-rich promoter sequences and substantially fewer enrichment peaks were observed on exon, intron, UTR, and intragenic regions. As shown in Fig. 1A (left panel), 13,227 enrichment peaks (*P*-values from $< 10^{-5}$ to $< 10^{-20}$) for OGG1 were identified at 30 min. In comparison, NF-κB was recruited to 8741 cis-acting target sequences on a genome-wide scale (Fig. 1A, right panel). For example, at 30 min post-exposure, in a 1,000-bp range, 45.1% of OGG1's enrichment peaks were localized to promoters-TSS, 28.3% to introns, and 15.2% to exons. There were low numbers of enrichment peaks of OGG1 on intergenic (4.2%), 5'UTR (4.1%), 3'UTR (0.6%), and other non-coding (2.3%) genomic regions (Fig. 1B, left panel). The distribution of NF-κB enrichment peaks are in line with previous observations [48]. Strikingly, the distribution of OGG1 enrichment peaks are similar to those of NF-κB at 1000 bp or longer (2000, or 10,000 bp ± TSS) genomic region (Fig. 1B, right panel). Moreover, the allocation of the OGG1 and NF-κB enrichment peaks relative to TSS (between +2000 and −2000 bp) are similar (Fig. 1C, upper and lower panels). Of note, the Homer motif discovery program did not identify any specific genomic sequence element for OGG1, suggesting that its enrichment on DNA occurs at its genomic substrate, 8-oxoG (or FapyG).

To examine whether OGG1 Ab-ChIP-ed genes are attributed to biological processes, system level analyses were performed using Gene Ontology (GO) enRIchment anaLysis and visuaLizAtion tool (GOrilla) [41]. To do so, a ranked list of genes (peak scores $< 10^{-5}$) was submitted to Gorilla. The results are summarized in Fig. 1D and Supplementary Table 1. GO analysis showed that OGG1-ChIP-ed genes are involved in various biological processes, including responses to oxidative stress (P = 1.04E-23), cellular redox homeostasis (P = 2.30E-12), regulation of cellular response to oxidative stress (P = 7.24E-09), and negative regulation of programmed cell death (P = 1.97E-11). GO analysis also revealed that OGG1 Ab ChIP-ed genes are involved in positive regulation of cellular metabolic process (P = 4.15E-09), mitochondrial function [mitochondrial membrane potential (4.84E-08) and depolarization (P = 4.51E-07)], and regulation of inflammatory responses (P = 5.51E-07). These biological processes are driven at the transcriptional level [DNA-templated transcription (P = 1.95E-08), transcription from RNA polymerase II dependent promoters (P = 2.55E-09), the positive regulation of gene expression (P = 1.03E-07)] (Fig. 1D). These results together are supported by data that showed an increased susceptibility to obesity and related pathologies [16,17], aberrant innate and adaptive immune responses in *Ogg1*$^{-/-}$ mice [13,14,19,46], developmental abnormalities of the central nervous and cardiovascular system in *Ogg1* deficient zebrafish [47,48], and aging processes [49].

3.2. Enrichment peaks of OGG1 are primarily located at gene regulatory regions

A representative segment of chromatin (chromosome (Crh) 4: 73836556 bp to 73998729 bp) with a cluster of 5 genes was selected to visualize OGG1's enrichment peaks using Integrative Genomics Viewer (IGV, Materials and Methods) and human genome-38 as reference (Fig. 2A). Visualization by IVG showed that the enrichment peaks of OGG1 were located at 5' end of each genes encoding the C-X-C motif chemokine ligand 6 (*CXCL6*), platelet factor 4 variant 1 (*PF4V1*), C-X-C motif chemokine ligand 1 (*CXCL1*), platelet factor 4 (*PF4*), and C-X-C motif chemokine ligand 5 (*CXCL5*) (Fig. 2A). Intriguingly, there was no or low level of OGG1 enrichment observed on intergenic and coding regions. In controls, enrichment peaks of the sequence-specific NF-κB are localized to the 5' end of genes, similar to OGG1. To visualize genomic locations of enrichment peaks at higher resolution, we selected C-C motif chemokine ligand 20 (*CCL20*), *CXCL1*, and interleukin 6 (*IL6*) (Fig. 2B, C, D), as well as *CXCL5*, *CXCL6,* nuclear factor-kappa-B p65 subunit *(RELA)*, lymphotoxin alpha (*LTA*), intercellular adhesion

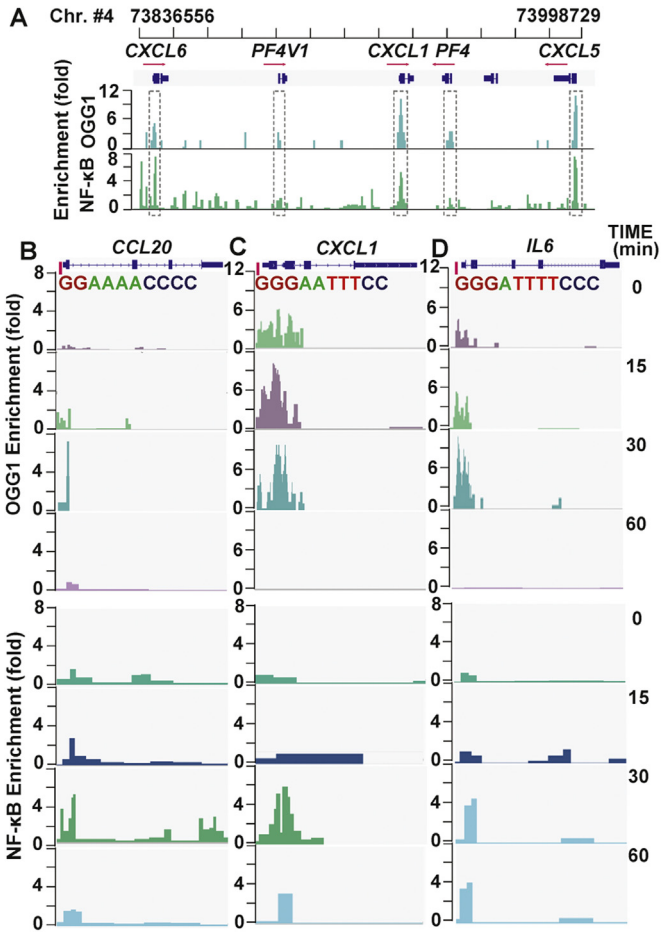

Fig. 2. Visual depiction of OGG1's enrichment peaks on promoters of selected genes in cells exposed to TNFα-ROS. A. Genome browser tracks showing enrichment of OGG1 (upper panel) and NF-κB (lower panel) on clusters of genes located on chromosome 4 (from 73836556–73998729 bp). Arrows indicate directions of transcription. B, C, D, OGG1 enrichment is primarily localized to gene regulatory regions and it is time-dependent (upper panels). Lower panels show the location of NF-κB's enrichment peaks. Examples shown include *CCL20* (chr #2: 227,813,854 - 227,817,534 bp); *CXCL1* (chr #4: 73,869,404 - 73,871,242 bp); and *IL6* (chr #7: 22,727,146 - 22,732,002 bp). A, B, C, D, Images were directly taken from IGV. Chr, chromosome; *CXCL6, chemokine (C-X-C motif) ligand 6*, *PF4V1*, platelet factor 4 variant (C-X-C motif chemokine 4), *PF4*, platelet factor 4 precursor also called C-X-C motif ligand 4 (CXCL4); *CCL20*, C-C motif chemokine ligand 20; *CXCL1*, C-X-C motif chemokine ligand 1; *IL6*, interleukin 6. IGV, integrative genome viewer.

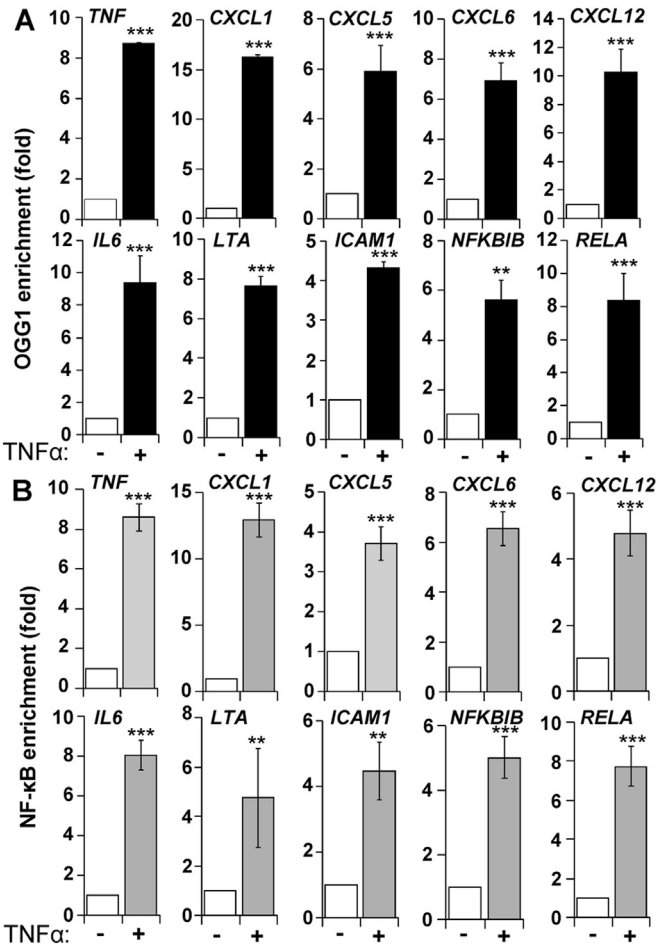

Fig. 3. Stimuli-driven enrichment of OGG1 and NF-κB is shown on TSS adjacent promoter regions. A, Enrichment of OGG1 on promoter regions of selected pro-inflammatory genes. B, NF-κB's enrichment on DNA in response to TNFα-ROS. In A and B, cells were exposed to TNFα for 30 min, DNAs were ChIP-ed with Ab to FLAG(OGG1) or RelA(NF-κB) and the genomic regions were PCR-amplified (Materials and Methods) (n = 3). Fold changes were calculated as described in Materials and Methods [37]. $^{**}p < 0.01$, $^{***}p < 0.001$. *TNF*, tumor necrosis factor; *CXCL1*, C-X-C motif chemokine ligand 1; *CXCL5*, C-X-C motif chemokine ligand 5; *CXCL6*, C-X-C motif chemokine ligand 6; *CXCL12*, C-X-C motif chemokine ligand 12; *IL6*, interleukin 6; *LTA*, lymphotoxin alpha (TNF superfamily, member 1); *ICAM*, intercellular adhesion molecule 1; *NFKBIB*, NF-κB inhibitor beta; *RELA*, v-Rel avian reticuloendotheliosis viral oncogene homolog A, an NF-κB subunit.

molecule 1 (*ICAM1*), C-X-C motif chemokine ligand 12 (*CXCL12)*, and NF-kappa-B inhibitor beta (*NFKBIB)* (Supplementary Fig. 1 and 2). OGG1 enrichment on nerve growth factor (*NGF*) is shown as an example of a non-inflammatory gene (Supplementary Fig. 2). Results showed that enrichment peaks of OGG1 were primarily localized to TSS-adjacent regulatory sequences and fold changes in the enrichment were time-dependent. There were one only of two scenarios observed for the OGG1 enrichment at time 0: either 1) a lack of, or insignificant levels of OGG1 enrichment (Fig. 2B), or 2) OGG1 was already present on TSS-adjacent promoter regions (Fig. 2C, D, upper panels). A typical example for the scenario #1 is the *TNF* promoter itself, as we documented previously [33], or *CCL20 of which* the enrichment of OGG1 on regulatory region was 0.1–0.8-fold over the background (Fig. 2B). Scenario #2 is valid for a greater portion of the tested genes: OGG1 was present to varying extents in the proximal promoter regions at time 0 (Fig. 2C, D and Supplementary Fig. 1,2). Importantly, the enrichment of OGG1 was increased from 15 min onward (for both scenarios). Taking *CXCL1* and *IL6* genes as examples, a 3- to 4-fold enrichment of OGG1 was observed at 15 min, which further increased to 12- to 14-fold over background by 30 min (Fig. 2C, D). In the case of NF-κB, low level enrichment was seen at time 0; however, from 15 min post-exposure, it gradually enriched, showing a maximum at 30 min (3- to 5-fold over background) in response to TNFα-ROS exposure. As expected, the NF-κB enrichment peaks aligned with its putative genomic binding sites (Fig. 2B, C, D, lower panels). At 60 min, OGG1 at proximal promoter regions was under the detectable level, while NF-κB enrichments persisted and were 2- to 4-fold (Fig. 2B, C, D and Supplementary Fig. 1,2).

To confirm the enrichment of OGG1 at TSS-adjacent genomic regions, we designed primers based on the genomic sequences surrounding OGG1's enrichment peaks. We also considered the proximity of the putative NF-κB binding sites (e.g., 5-GGG*RNYYY*CC-3; in which *R* is purine, *Y* is pyrimidine, and *N* can be any nucleotide; [50]) as OGG1 facilitates DNA occupancy of transcription factors including NF-κB [32,33]. The sequences of validated primer pairs are shown in Table 1 (Materials and Methods). The parallel cultures of FLAG-OGG1-expressing cells were mock- or exposed to TNFα-ROS for 30 min, and ChIPs

were carried out using Ab to FLAG(OGG1). For controls, ChIPs were performed using Ab to RelA(NF-κB). As shown in Fig. 3A, in response to TNFα-ROS exposure, OGG1 showed an average enrichment of 8.8-, 17.5-, 5.9-, 7.1-, 10.5-, 9.2-, 7.8-, 4.4-, 5.5-, and 8.2-fold compared to mock-exposed cells for *TNF, CXCL1, CXCL5, CXCL6, CXCL12, IL6, LTA, ICAM1, NFKBIB, and RELA,* respectively (Fig. 3A). These results strongly support and complement the data shown in Fig. 2B and Supplementary Fig. 1,2. For the controls, increases in NF-κB's enrichment on these genomic regions (Fig. 3B) are consistent with the presence of its binding sites [45,51].

3.3. OGG1 enrichment on chromatinized DNA is functional

Ogg1$^{-/-}$ mice show aberrant immune responses [13,14,46] and our system level analysis using Gorilla identified the regulation of immune responses as a highly significant GO category (Fig. 1D). Thus, we next examined the significance of OGG1 Ab ChIP-ed genes in the immune responses. We first collected all the genes that had previously been associated with innate immune response (IIR) by using the GeneCards database (Materials and Methods). The list consisting of 1294 IIR genes was "overlaid" onto the OGG1 Ab-ChIP-ed genes, out of which 840 were identical. In controls, 769 NF-κB Ab ChIP-ed genes were present among the 1294 genes identified by GeneCards. The results showed that 673 (80%) genes were present in both the OGG1-Ab-ChIP-ed and NF-κB-Ab-ChIP-ed genes, whereas 167 and 96 were unique to each, respectively (Fig. 4A). The majority of OGG1 and NF-κB enrichment peaks were found on promoter-TSS (392 OGG1 and 373 NF-κB) and exon I (277 OGG1 and 249 NF-κB), whereas substantial differences were observed between OGG1 and NF-κB in their enrichment at 5'UTR and introns (Fig. 4B). To gain further insight into the major GO categories associated with the OGG1-ChIP-ed genes, the ranked list of 840 IIR genes (peak scores from $< 10^{-5}$ to 10^{-20}) was submitted to GOrilla [41]. Results showed that OGG1-ChIP-ed genes are most significantly related to the host defense response (P = 7.76E-19), immune system processes (P = 1.82E-15), inflammatory response (P = 2.34E-14), response to biotic stimulus (P = 7.32E-14), defense response to other organisms (P = 2.10E-13), and response to external biotic stimulus (P = 3.32E-13) (Fig. 4C, Supplementary Table 2). Moreover, the hierarchical structure and relationship among enriched GO terms showed that IIR processes manifest via generation and secretion of soluble mediators (cytokines, chemokines, and ILs) (Fig. 4D; over-representation levels are expressed as –log (P value)) and colour coded). The most significantly modulated processes involve the positive regulation of cytokine production (P = 1.81E-10), including TNFα (P = 3.18E-06), IL6 (interferon, beta 2; P = 3.62E-07), C-X-C motif chemokine ligand 8 (IL8) (P = 1.39E-07), and interleukin-1 production (P = 3.22E-06). The heterodimeric interleukin 23 (IL23, 3.34E-04) and IL-17 (P = 1.4E-04) were also significantly modulated. These data are in line with the enrichment of OGG1 on regulatory regions of *CXCLs*, *CCLs*, and *ILs* (Figs. 2, 3 and Supplementary Fig. 1,2) as well as those showing aberrant immune response to challenge of *Ogg1*$^{-/-}$ mice [13,14,19,52,53]. As expected from previous studies [51] NF-κB-ChIP-ed genes are associated with IIR signaling pathway(s) (Supplementary Fig. 3,4).

Next, we examined the functional significance of TNFα-generated ROS-induced OGG1's enrichment on gene regulatory sequences (Figs. 1,2,3). To do so, OGG1 was siRNA-depleted or not and cells were mock- or TNFα-ROS exposed for 1 h [time point is previously defined [32,52]. RNAs were isolated and changes in mRNA levels were determined utilizing human inflammatory cytokines and receptors array (Materials and Methods). The expression of numerous pro-inflammatory chemokines and cytokines was significantly increased in TNFα-ROS-exposed cells compared to that of mock-treated ones. At 1 h post exposure, increases in mRNA levels of *CCL20, CXCL1, CXCL2, CXCL3, CXCL5, CXCL8, CXCR1,* and *TNF* were 11.7-, 87.7-, 30.8-, 18.7-, 6.8-, 20.7-, 5.1-, and 21.9–fold, respectively. mRNA levels for other

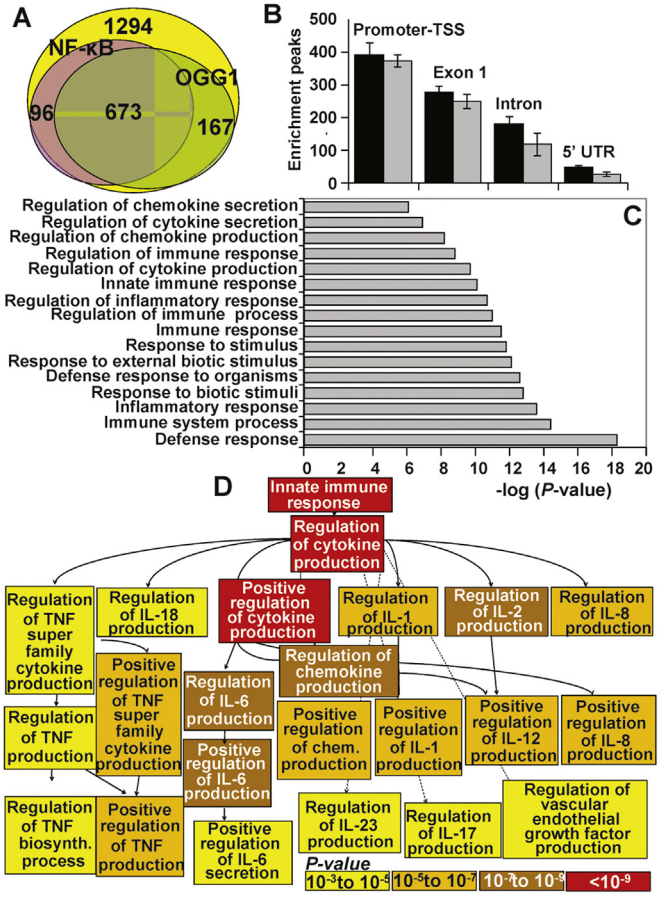

Fig. 4. Location of OGG1 and NF-κB enrichment peaks and overrepresented IIR processes associated with OGG1 Ab-ChIP-ed genes. **A**, Unique and overlapping genes ChIP-ed by OGG1- and RelA(NF-κB)-Abs in the IIR pathway. IIR genes (1294) identified by GeneCards database was "overlaid" onto the OGG1 and NF-κB Ab-ChIP-ed genes. **B**, Genomic location of OGG1 and NF-κB enrichment peaks in the IIR genes. **C**, Gene ontology categories defined by Gorilla, based on OGG1 ChIP-ed genes. The ranked list of genes was submitted to GOrilla online system, and the GOrilla-defined overrepresentation levels of each biological process are expressed as –log (P value), as depicted utilizing the Microsoft Excel program. **D**, A hierarchical structure and relationship among enriched gene ontology (GO) terms based on OGG1-Ab ChIP-ed IIR genes. Genes were ranked according to their peak score and given as input to GOrilla. The resulting GO terms were visualized by using a DAG graphical representation tool with color coding reflecting the degree of enrichment [41]. GOrilla, gene ontology enRIchment anaLysis and visuaLizAtion system; IIR, innate immune response; 5'UTR, five prime un-translated region.

inflammatory mediators and receptors did not significantly change at this time point (Fig. 5A). The siRNA depletion of OGG1 significantly decreased the extent of TNFα-ROS induced pro-inflammatory gene expression. Results summarized in Fig. 5B show decreased mRNA levels of *CCL20* (from 11.7- to 0.5-fold), *CXCL1* (from 87.7- to 3.9-fold), *CXCL8* (from 20.7- to 2.2-fold), *CXCL5* (from 6.8- to 1.0-fold), *CXCL2* (from 30.8- to 3.7-fold), and *TNF* (from 21.9- to 2.8-fold). Interestingly, mRNA levels of *CXCL3* were not altered, compared with levels in the OGG1-expressing cells (Fig. 5B; Supplementary Table 1). To confirm these results, changes in gene expression levels were assessed for selected genes (*TNF, CXCL1, CXCL3,* and *CXCL8)* by individual qRT-PCR (Fig. 5D,E,F,G). Of note, OGG1 depletion resulted in a decreased basal expression of 62 out of 86 inflammatory genes, while the expression of 5 out of 86 genes was increased by 2–2.5-fold compared to that in mock-treated OGG1 proficient cells (Fig. 5C, Supplementary Table 1). A three-dimensional illustration of these data is shown in Supplementary Fig. 3. Fig. 5H documents the levels of OGG1 at mRNA and protein

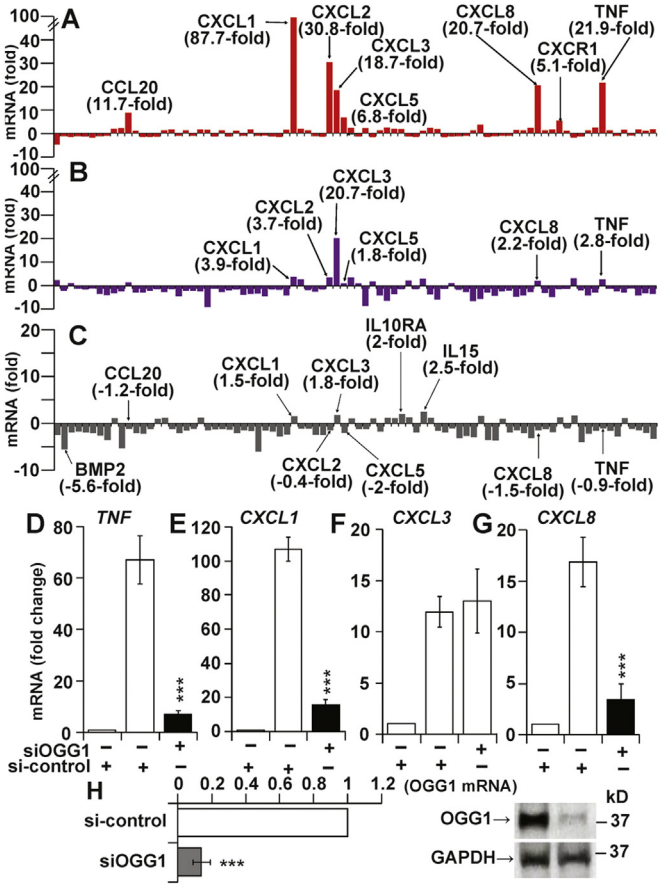

Fig. 5. OGG1 modulates the expression of pro-inflammatory mediators. A, TNFα-induced expression of pro-inflammatory mediators in OGG1-expressing cells. B, TNFα-induced expression of inflammatory chemokines and cytokines, in OGG1-depleted cells. C, Lack of OGG1 impact the basal expression of chemokines and cytokines. In A and C, cells were OGG1-depleted by siRNA and cells in B and C were exposed to TNFα (20 ng per ml) for 30 min. In A,B,C, changes in gene expression were determined using the human inflammatory cytokines and receptors array (Materials and Methods). D, E,F,G) Expression of *TNF*, *CXCL1, CXCL3 and CXCL8* as a function of OGG1 expression assessed by individual qRT-PCR. H, *OGG1* mRNA and protein levels prior and after the siRNA silencing of OGG1. In A to H, fold changes in gene expression were calculated by the $2^{-\Delta\Delta CT}$ method and normalized with GAPDH. **** $p < 0.001$. *CXCL1, Chemokine (C-X-C motif) ligand 1; CCL20, Chemokine (C-C motif) ligand 20; CCL2, Chemokine (C-C motif) ligand 2; TNF, Tumor necrosis factor; CXCL2, Chemokine (C-X-C motif) ligand 3, CXCL3, Chemokine (C-X-C motif) ligand 3; CXCL12, Chemokine (C-X-C motif) ligand 8; CXCL5, Chemokine (C-X-C motif) ligand 5; CXCL2, Chemokine (C-X-C motif) ligand 2.* Fold changes in mRNA levels are shown in Supplementary Table 1.

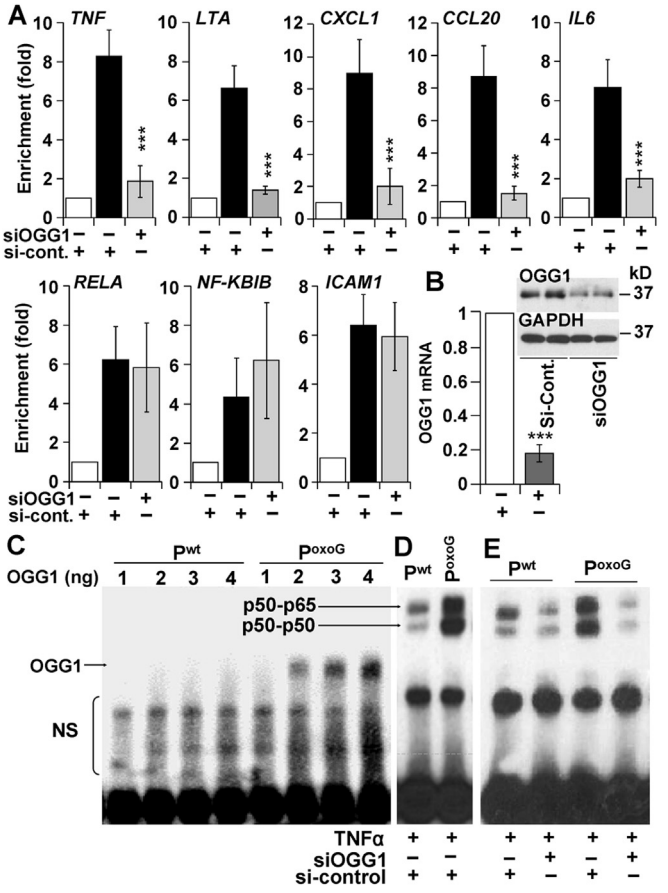

Fig. 6. Role of OGG1 in NF-κB's DNA occupancy in the chromatin and in vitro. A, OGG1 modulates DNA occupancy of NF-κB in the chromatinized DNA. Cells were OGG1-depleted or not and TNFα-exposed for 30 min. DNA was ChIP-ed by using RelA(NF-κB) Ab and subjected to q-PCR. Results are expressed as the fold enrichment relative to the IgG control. Fold changes were calculated as described in Materials and Methods [36]. B, Expression of OGG1 at the RNA and protein levels prior to and after *OGG1* siRNA depletion. *** $p < 0.001$. C, OGG1 binds exclusively to DNA containing 8-oxoG. D, Binding of NF-κB from crude nuclear extracts of TNFα-exposed cells to DNA containing its consensus sequence in the lack (P^{wt}) and presence of 8-oxoG (P^{oxoG}). E, Binding site occupancy of NF-κB is OGG1-dependent in crude nuclear extracts. DNA occupancy of NF-κB from NEs isolated from OGG1-expressing (si-*cont*) and OGG1-depleted (si*OGG1*) TNFα-exposed cells onto P^{WT} and P^{oxoG} probes. Electromobility shift assays (EMSA) were performed as described in Materials and Methods. P, probe; *TNF,* Tumor necrosis factor; *LTA,* Lymphotoxin alpha (TNF superfamily, member 1); *CXCL1,* Chemokine (C-X-C motif) ligand 1*; CCL20,* Chemokine (C-C motif) ligand 20*; IL6,* interleukin 6; *RELA*, v-Rel avian reticuloendotheliosis viral oncogene homolog A, an NF-κB subunit; *NFKBIB*, NF-κB inhibitor beta; *ICAM*, Intercellular adhesion molecule 1.

levels prior and after si*OGG1*-mediated depletion. Taken together, these data imply that the enrichment of OGG1 on gene regulatory regions has important functions in induced expression of genes.

3.4. Chromatin-associated OGG1 acts jointly with transacting factors for efficient gene expression

The gene ontology enrichment analysis identified a highly significant association of OGG1 ChIP-ed genes with DNA-templated transcription from RNA polymerase II dependent promoters, suggesting key roles for products from OGG1 modulated genes in regulation of gene expression (Fig. 1D). To build on these observations, we tested whether products of OGG1 Ab ChIP-ed genes are involved in the activation and DNA binding of sequence-specific binding proteins by means of NF-κB as an example. The ranked list of genes ChIP-ed by both OGG1 and NF-κB Abs in the IIR pathway (Fig. 4A) was submitted for GO analysis by using GOrilla visualization system. The results showed that OGG1 Ab ChIP-ed genes are involved in signal transduction, positive regulation of I-κB kinase and NF-κB transcription factor activity, NF-κB's post-translational modification, transcription factor import into the nucleus, and the sequence-specific DNA binding of transcription factor activity (Supplementary Fig. 6)

To associate these observations with close proximity of enrichment peaks of OGG1 and NF-κB (Fig. 2), we tested whether OGG1 plays a role in the DNA occupancy of NF-κB in the chromatin. Cells were OGG1-depleted by siRNA or not (control siRNA) and exposed to TNFα-ROS for 30 min; then DNAs were ChIP-ed with RelA(NF-κB) Ab. Results from ChIPs showed (Fig. 6A) OGG1 depletion decreased in NF-κB's DNA enrichments for *LTA*, *IL6*, *CCL20*, *TNF*, *CXCL1*, and *CXCL6,* but it had no significant effect on *RELA, NF-KBIB*, and *ICAM1*. Fig. 6B shows the expression of OGG1 prior to and after siRNA depletion. These data

complement the results showing down-regulation, up-regulation, or no effect of OGG1 on gene expression (Fig. 5, Supplementary Table 1). Although additional work is required, these data strongly suggest that the binding of OGG1 to its genomic substrate 8-oxoG, as well as gene products regulated by OGG1, modulate DNA occupancy of transcription factors in the chromatin. To this end, in addition to NF-κB, numerous additional transcription factor binding motifs were identified in proximity to OGG1 enrichment sites (-log *P*-values are between 1e-797 and 1e-10; Supplementary Table 4).

To obtain evidence for interaction of OGG1 with DNA at 8-oxoG, we performed electrophoretic mobility shift assay (EMSA) using wild-type synthetic DNA (probe: P^{WT}) and an 8-oxoG-containing probe (P^{oxoG}). These probes also contained guanine-rich NF-κB binding motif (5'-GGGGTATCC-3') [50,54]. 8-OxoG was placed upstream (8 bp) from the NF-κB motif (Materials and Methods and as we described previously [33]). As shown in Fig. 6C, OGG1 did not bind to P^{WT}, while it did bind specifically to P^{oxoG} in a concentration-dependent manner (Fig. 6C). These results support the hypothesis that the enrichment of OGG1 in the promoter region occurs at 8-oxoG in the chromatin. To test whether OGG1-DNA interaction at 8-oxoG increases DNA occupancy of transcription factor(s), nuclear extracts (NE) were isolated from OGG1-expressing cells and NF-κB binding to P^{WT} and P^{oxoG} was examined by using EMSA. NF-κB's DNA occupancy was excessive on the probe containing 8-oxoG compared to that on P^{WT} (Fig. 6D). NF-κB binding to P^{WT} in NEs isolated from OGG1-depleted TNFα-ROS-stimulated cells was slightly affected, while its DNA occupancy on the probe containing 8-oxoG was decreased nearly to a level similar to that observed on P^{WT} (Fig. 6E). Together, these data suggest that the enrichment of OGG1 in the proximity of NF-κB binding sites facilitates sequence occupancy of NF-κB in the chromatin.

4. Discussion

OGG1 is the primary enzyme that initiates repair of oxidatively modified guanine base lesions including 8-oxoG and FapyG (reviewed in [55]). Recent evidence also suggests that 8-oxoG has an epigenetic role and OGG1 is a modulator of gene expression [18,20,21,23–25,31–33,56]. Here, for the first time, we document a TNFα-stimulated, ROS-dependent enrichment of OGG1 on specific genomic regions of the chromatinized DNA. Nearly half of the OGG1 enrichment peaks were localized to TSS-adjacent regulatory regions, which was limited to a time scale required for prompt cellular responses. OGG1 enrichment on these specific regions of chromatin is functional as shown by OGG1's impacts on NF-κB's DNA occupancy and differential gene expression. System level analysis implied that OGG1-ChIP-ed genes are primarily involved in the regulation of cellular responses to oxidative stress, and cellular redox homeostasis that can potentially affect complex physiological and patho-physiological cellular biological processes. Together, these data demonstrate that the ROS-driven enrichment of OGG1 at specific sites of the chromatin is a prerequisite to gene expression, for prompt cellular responses to oxidative stress.

Results from ChIP sequence alignment analysis revealed that nearly half of OGG1 enrichment peaks were localized to TSS-adjacent regulatory regions; however, the Homer motif discovery program failed to identify specific genomic sequence element(s) for OGG1 binding, suggesting that its DNA interactions may occur at its genomic substrate(s). This hypothesis is in line with the observed preferential increase in levels of 8-oxoG lesions within proximal, but not distal, promoter regions both in human and mouse cells after TNFα-ROS exposure as shown by Flare-qPCR [32–34]. This possibility is also supported by our previous data, showing that preventing guanine oxidation in TNFα-exposed cells decreased OGG1 enrichment to background levels [32–34]. Ding and his colleagues have identified regions of the genome that are less protected from ROS, primarily in the promoter and UTR regulatory regions acquiring greater levels of 8-oxoG and increased OGG1 binding [30]. Studies by Dr. Gillespie's lab showed that the physiologically relevant ROS induced by hypoxia resulted in accumulation of 8-oxoG and OGG1 in functionally active promoters including vascular endothelial growth factor (VEGF), whereas the promoter regions of genes not involved in hypoxia response failed to display oxidative guanine modifications [21–23]. Fleming and his colleagues have elegantly documented that non-random guanine oxidation to 8-oxoG and OGG1 binding were guided to potential guanine quadruplexes upstream from TSS [31].

OGG1's interaction with its substrate in the genomic DNA primarily occurred at gene regulatory regions as evidenced by sequence alignment and it was gradual between time 0 and 30 min. DNA occupancy for an extended time period was unusual as previous studies performed in vitro showed that the repair of 8-oxoG follows a single-exponential time course and the observed excision rate constant with substrate-containing DNA varied between $0.49\,s^{-1}$ and $0.74\,s^{-1}$ [57]. Even though OGG1's turnover on substrate-containing DNA was somewhat dependent on the DNA sequence in neighboring regions, the repair time was within a time range of seconds [57,58]. The prolonged association of OGG1 with genomic regions may be explained by its inability to excise its substrate(s) possibly due to supra-physiological levels of ROS in TNFa-exposed cells. Bravard and his colleagues documented that oxidative inactivation of OGG1's enzymatic activity occurs mainly by direct oxidation at critical cysteine residues and both its glycosylase and AP-lyase activities are restored along with the normalization of the cellular redox status [59]. In our follow up studies, oxidatively modified OGG1 at cysteine(s) was detected in nuclear extracts of TNFα-exposed cells using biotin-linked trapping reagent that specifically reacts with cysteine sulfenic acid [32,33]. Another study showed inactivation of OGG1 at cysteine 326 with simultaneous increases in genomic 8-oxoG levels by physiologically relevant levels of TNFα-ROS [42]. Taking these observations together, one may hypothesize that the enrichment of OGG1 on chromatinized DNA likely at its substrate for a prolonged period of time is due to the loss of its enzymatic activity by ROS *in cellulo*.

Enrichment of OGG1 on gene regulatory regions has important roles in modulation of gene expression. Specifically, results showed that both basal and induced expression of cytokines, chemokines and their receptors were altered (primarily decreased) in OGG1-depleted cultured cells after TNFa-ROS exposure. Although distantly, these data are in line with the aberrant/decreased expression of pro-inflammatory mediators as well as the innate and allergic immune responses observed in *Ogg1*$^{-/-}$ mice challenged with TNFα, bacterial endotoxin, allergens, or infected with bacterial pathogens (*Helicobacter pylori*, *Pseudomonas aeruginosa*) [13–15,46,52,60]. Both innate and adaptive immune process(es) are regulated by hierarchically organized set of molecular, cellular, and organismal networks driven by large numbers of genes. Indeed, among the nearly 1300 genes in the IIR pathway, 840 were present in OGG1 Ab-ChIP-ed genes as identified by one of the most authentic database GeneCards. In comparison, we found nearly identical numbers of genes ChIP-ed by RelA(NF-κB) Ab in the same list, providing high level of confidence in our data as NF-κB is one of the master regulator of inflammatory gene expression [45]. Our system level analysis revealed that the molecular functions of OGG1 Ab-ChIP-ed genes are involved in host defense responses, and immune system processes, which are manifested through differential gene expression and secretion of soluble mediators (cytokines, chemokines, and interleukins). Here, we have analyzed only role of OGG1 in the IIR networks; however, using microarray technology, Dr. Lloyd's lab found differentially expressed family of genes in hepatocytes and muscles of *Ogg1*$^{-/-}$ compared to *Ogg1*$^{+/+}$ mice prior to and after high fat feeding [16,17]. The authors concluded that OGG1 may be linked to the expression of genes involved in cellular metabolism, because there were no notable differences in 8-oxoG levels in genomic and mitochondrial DNA prior to and after development of metabolic disorders [16,17]. Although the cell type used in our studies is different from muscle or liver hepatocytes,

our system level analysis still identified a highly significant association of OGG1 Ab ChIP-ed genes with regulation of metabolic processes and mitochondrial functions, including regulation of mitochondrial membrane potential and depolarization.

Binding sequence(s) exclusive for OGG1 cannot be identified, raising the possibility that OGG1 may bind its genomic substrate, 8-oxoG and regulate transacting factor's DNA occupancy concomitantly [21,23,26,32–34]. This hypothesis is supported by our observations that distribution and location of OGG1's enrichment peaks are in close proximity to those sequences, which are recognized by the sequence-specific binding protein NF-κB. In support, OGG1-depletion led to modulation of NF-κB sequence binding; a decrease in enrichment of NF-κB was observed in promoter regions of *TNF*, *CXCL1*, *IL6*, *LTA*, and IL*6*. These observations along with those published previously, imply a role for OGG1 in modulation of transcription factor's (NF-κB, HIF, VEGF, MYC, and SP1) DNA occupancy [21,25,31–33]. Recent studies have documented that in the nuclear extract or in mixture with recombinant NF-κB subunits, OGG1 increased the DNA binding of homo- and heterodimeric NF-κB when 8-oxoG was synthetically inserted into DNA probes [33,34]. The increases in NF-κB DNA binding exceeded 25-fold, and it was hypothesised that OGG1, by flipping 8-oxoG out of the DNA double helix and interacting with the opposite cytosine, creates changes in adjacent DNA architecture and facilitates NF-κB's DNA occupancy [34]. Of note, the DNA structural changes that occur during base flipping take place in the presence of OGG1 and DNA, requiring neither base excision nor generation of an AP site [61,62]. Localized structural changes in DNA is a universal feature of bacterial and eukaryotic DNA glycosylases (e.g., Fpg, OGG1, NEILs) [55,61–63] thus modulation of transcription factor binding may not be unique to OGG1. For example, NEIL2 decreased NF-κB's DNA occupancy on synthetic DNA or in chromatin [32,33]. In line with these observations, a recent study showed significantly increased inflammatory responses of *Neil2*$^{-/-}$ mice to ROS, LPS, or TNFα compared to wild-type mice [64]. Because deletion of *Neil2* has no effect on expression of OGG1, these data can also be interpreted as that NEIL2 opposes OGG1's pro-transcriptional, pro-inflammatory actions [64].

According to the present knowledge, OGG1 modulates gene expression via a process that involves its substrate binding with or without involvement of its enzymatic activity [18,20,65]. Dr. Burrows' lab documented that increased gene expression occurs when 8-oxoG is excised and AP sites are generated by OGG1 within G-quadruplex–forming sequences in promoters of VGEF and endonuclease III-like protein [29–31]. The scenario involving excision of 8-oxoG and further generation of strand break by OGG1 was shown to be the entry point for topoisomerase II beta (Top IIβ), which mediates DNA conformational changes, leading to estrogen-induced gene expression from the apoptosis regulator *BCL*-2 or breast cancer estrogen-inducible protein-2 promoters [24]. Similarly, 8-oxoG excision by OGG1 was instrumental in MYC-, retinoic acid-, sirtuin-1, and androgen-driven transcription of genes [25–27]. In contrast, a series of papers documented that the interaction of the enzymatically inactive OGG1 with DNA at its substrate 8-oxoG was sufficient to prompt expression of chemokines and cytokines [19,33,34]. On the other hand, OGG1 was implicated in epigenetic suppression of gene expression for multiple genes via DNA hypermethylation. Xia and colleagues documented that the chromodomain helicase DNA binding protein 4 (CHD4) is recruited by OGG1 bound to genomic 8-oxoG. OGG1-CHD4 complex mediated the recruitment of DNA methyltransferases leading to DNA hypermethylation, consequently to transcriptional silencing of tumor suppressor genes [66]. A recent study documented a role for OGG1 in symmetric dimethylation of histone H4 arginine-3 (H4R3me2s). Specifically, OGG1 at its DNA substrate recruits protein arginine N-methyltransferase 5 (PRMT5), which catalyzes symmetrical dimethylation on arginine-3 and results in gene silencing [67]. Of note, Dr. Ba and her colleagues aligned OGG1 enrichment peaks identified by our ChIP-seq analysis with both hypo- and hyper- methylated sites on the chromatinized DNA (manuscripts in preparation).

5. Conclusion

Oxidative modification to DNA strands and nucleobases -induced or accidental- is associated with unfavorable consequences, including mutations or loss/gain in genetic information, which are prevented by DNA repair proteins. However, mounting recent data support the hypothesis that some of the genomic base modifications primarily 8-oxoguanine along with the cognate repair protein OGG1 has distinct roles in gene expression. In light of these data, we performed ChIP-coupled sequencing and made advances by showing TNFα-induced, ROS-driven enrichment of OGG1 at specific regulatory regions of large numbers of genes in the chromatinized DNA. ChIP-sequence alignment analysis showed preferential promoter enrichment of OGG1 –located in close proximity of transcription factor's binding motifs. OGG1 at gene regulatory regions is functional as it modulates the binding of transacting factors and gene expression. It appears that ROS from intrinsic and extrinsic sources yield 8-oxoguanine in guanine-rich promoters, where it serves as an epigenetic mark, and the bound OGG1 provides a platform for the assembly of the transcriptional machinery to launch prompt and preferential expression of redox-regulated genes that modulate complex cellular physiological and biological processes.

Funding

This work was supported by grants from the National Institute of Environmental Health and Sciences RO1 ES018948 (IB); P30 ES006676 (IB), and T32 ES007254-22 (L.A-A), National Institute of Allergic and Infectious Diseases NIAID/AI062885 (IB, ARB). National Science Foundation of China (Grant No: 31571339 to XB and 81402338 to QT), National Scholarship Fund of China, Scholarship Council (Grant No. 201506175184 and 201606620041).

Acknowledgements

We thank Dr. Linsey A. Yeager (Institute for Human Infections and Immunity) for her scientific input and for editing the manuscript.

Conflict of interest

The authors declare that they have no conflict of interest

Author contributions

I.B. and X.B. designed the study. T.Q., L.P., W.H., LA. A., A.B. and SA.V. carried out the research experiments. I.B. and X.B. wrote the manuscript, and AR.B., SA.V., and Z.R. edited and gave scientific advice. All authors reviewed the results and approved the final version of the manuscript.

Appendix A. Supplementary material

Supplementary data associated with this article can be found in the online version at http://dx.doi.org/10.1016/j.redox.2018.06.002.

References

[1] S.S. David, V.L. O'Shea, S. Kundu, Base-excision repair of oxidative DNA damage, Nature 447 (2007) 941–950.
[2] S.P. Jackson, J. Bartek, The DNA-damage response in human biology and disease, Nature 461 (2009) 1071–1078.
[3] M. Dizdaroglu, Formation of an 8-hydroxyguanine moiety in deoxyribonucleic acid on gamma-irradiation in aqueous solution, Biochemistry 24 (1985) 4476–4481.
[4] C.J. Burrows, J.G. Muller, Oxidative nucleobase modifications leading to strand scission, Chem. Rev. 98 (1998) 1109–1152.
[5] S. Mitra, T. Izumi, I. Boldogh, K.K. Bhakat, J.W. Hill, T.K. Hazra, Choreography of oxidative damage repair in mammalian genomes, Free Radic. Biol. Med. 33 (2002)

15–28.
[6] M.L. Hegde, P. H, K.S. Rao, S. Mitra, Oxidative genome damage and its repair in neurodegenerative diseases: function of transition metals as a double-edged sword, J. Alzheimers Dis. 24 (2011) 183–198.
[7] T.K. Hazra, J.W. Hill, T. Izumi, S. Mitra, Multiple DNA glycosylases for repair of 8-oxoguanine and their potential in vivo functions, Prog. Nucleic Acid. Res Mol. Biol. 68 (2001) 193–205.
[8] M.L. Hegde, P.M. Hegde, L.J. Bellot, S.M. Mandal, T.K. Hazra, G.M. Li, I. Boldogh, A.E. Tomkinson, S. Mitra, Prereplicative repair of oxidized bases in the human genome is mediated by NEIL1 DNA glycosylase together with replication proteins, Proc. Natl. Acad. Sci. USA 110 (2014) E3090–E3099.
[9] M. Dizdaroglu, Base-excision repair of oxidative DNA damage by DNA glycosylases, Mutat. Res 591 (2005) 45–59.
[10] A. Klungland, I. Rosewell, S. Hollenbach, E. Larsen, G. Daly, B. Epe, E. Seeberg, T. Lindahl, D.E. Barnes, Accumulation of premutagenic DNA lesions in mice defective in removal of oxidative base damage, Proc. Natl. Acad. Sci. USA 96 (1999) 13300–13305.
[11] O. Minowa, T. Arai, M. Hirano, Y. Monden, S. Nakai, M. Fukuda, M. Itoh, H. Takano, Y. Hippou, H. Aburatani, K. Masumura, T. Nohmi, S. Nishimura, T. Noda, Mmh/Ogg1 gene inactivation results in accumulation of 8-hydroxyguanine in mice, Proc. Natl. Acad. Sci. USA 97 (2000) 4156–4161.
[12] T. Arai, V.P. Kelly, O. Minowa, T. Noda, S. Nishimura, The study using wild-type and Ogg1 knockout mice exposed to potassium bromate shows no tumor induction despite an extensive accumulation of 8-hydroxyguanine in kidney DNA, Toxicology 221 (2006) 179–186.
[13] J.G. Mabley, P. Pacher, A. Deb, R. Wallace, R.H. Elder, C. Szabo, Potential role for 8-oxoguanine DNA glycosylase in regulating inflammation, Faseb J. 19 (2005) 290–292.
[14] A. Bacsi, L. Aguilera-Aguirre, B. Szczesny, Z. Radak, T.K. Hazra, S. Sur, X. Ba, I. Boldogh, Down-regulation of 8-oxoguanine DNA glycosylase 1 expression in the airway epithelium ameliorates allergic lung inflammation, DNA Repair (Amst.) 12 (2013) 18–26.
[15] E. Touati, V. Michel, J.M. Thiberge, P. Ave, M. Huerre, F. Bourgade, A. Klungland, A. Labigne, Deficiency in OGG1 protects against inflammation and mutagenic effects associated with H. pylori infection in mouse, Helicobacter 11 (2006) 494–505.
[16] H. Sampath, V. Vartanian, M.R. Rollins, K. Sakumi, Y. Nakabeppu, R.S. Lloyd, 8-Oxoguanine DNA glycosylase (OGG1) deficiency increases susceptibility to obesity and metabolic dysfunction, PLoS One 7 (2012) e51697.
[17] V. Vartanian, J. Tumova, P. Dobrzyn, A. Dobrzyn, Y. Nakabeppu, R.S. Lloyd, H. Sampath, 8-oxoguanine DNA glycosylase (OGG1) deficiency elicits coordinated changes in lipid and mitochondrial metabolism in muscle, PLoS One 12 (2017) e0181687.
[18] M. Seifermann, B. Epe, Oxidatively generated base modifications in DNA: not only carcinogenic risk factor but also regulatory mark? **in press**, Free Radic. Biol. Med (2017) **in press**.
[19] X. Ba, L. Aguilera-Aguirre, Q.T. Rashid, A. Bacsi, Z. Radak, S. Sur, K. Hosoki, M.L. Hegde, I. Boldogh, The role of 8-oxoguanine DNA glycosylase-1 in inflammation, Int J. Mol. Sci. 15 (2014) 16975–16997.
[20] A.M. Fleming, C.J. Burrows, 8-Oxo-7,8-dihydroguanine, friend and foe: Epigenetic-like regulator versus initiator of mutagenesis, DNA Repair (Amst.) (2017).
[21] V. Pastukh, J.T. Roberts, D.W. Clark, G.C. Bardwell, M. Patel, A.B. Al-Mehdi, G.M. Borchert, M.N. Gillespie, An oxidative DNA "damage" and repair mechanism localized in the VEGF promoter is important for hypoxia-induced VEGF mRNA expression, Am. J. Physiol. Lung Cell Mol. Physiol. 309 (2015) L1367–L1375.
[22] V. Pastukh, M. Ruchko, O. Gorodnya, G.L. Wilson, M.N. Gillespie, Sequence-specific oxidative base modifications in hypoxia-inducible genes, Free Radic. Biol. Med. 43 (2007) 1616–1626.
[23] D.W. Clark, T. Phang, M.G. Edwards, M.W. Geraci, M.N. Gillespie, Promoter G-quadruplex sequences are targets for base oxidation and strand cleavage during hypoxia-induced transcription, Free Radic. Biol. Med 53 (2012) 51–59.
[24] B. Perillo, M.N. Ombra, A. Bertoni, C. Cuozzo, S. Sacchetti, A. Sasso, L. Chiariotti, A. Malorni, C. Abbondanza, E.V. Avvedimento, DNA oxidation as triggered by H3K9me2 demethylation drives estrogen-induced gene expression, Science 319 (2008) 202–206.
[25] S. Amente, A. Bertoni, A. Morano, L. Lania, E.V. Avvedimento, B. Majello, LSD1-mediated demethylation of histone H3 lysine 4 triggers Myc-induced transcription, Oncogene 29 (2011) 3691–3702.
[26] S. Amente, L. Lania, E.V. Avvedimento, B. Majello, DNA oxidation drives Myc mediated transcription, Cell Cycle 9 (2010) 3002–3004.
[27] C. Zuchegna, F. Aceto, A. Bertoni, A. Romano, B. Perillo, P. Laccetti, M.E. Gottesman, E.V. Avvedimento, A. Porcellini, Mechanism of retinoic acid-induced transcription: histone code, DNA oxidation and formation of chromatin loops, Nucleic Acids Res. 42 (2014) 11040–11055.
[28] M. Seifermann, A. Ulges, T. Bopp, S. Melcea, A. Schafer, S. Oka, Y. Nakabeppu, A. Klungland, C. Niehrs, B. Epe, Role of the DNA repair glycosylase OGG1 in the activation of murine splenocytes, DNA Repair (Amst.) 58 (2017) 13–20.
[29] A.M. Fleming, J. Zhou, S.S. Wallace, C.J. Burrows, A role for the fifth G-Track in G-Quadruplex forming oncogene promoter sequences during oxidative stress: do these "spare tires" have an evolved function? ACS Cent. Sci. 1 (2015) 226–233.
[30] Y. Ding, A.M. Fleming, C.J. Burrows, Sequencing the mouse genome for the oxidatively modified base 8-Oxo-7,8-dihydroguanine by OG-Seq, J. Am. Chem. Soc. 139 (2017) 2569–2572.
[31] A.M. Fleming, Y. Ding, C.J. Burrows, Oxidative DNA damage is epigenetic by regulating gene transcription via base excision repair, Proc. Natl. Acad. Sci. USA 114 (2017) 2604–2609.
[32] X. Ba, A. Bacsi, J. Luo, L. Aguilera-Aguirre, X. Zeng, Z. Radak, A.R. Brasier, I. Boldogh, 8-oxoguanine DNA glycosylase-1 augments proinflammatory gene expression by facilitating the recruitment of site-specific transcription factors, J. Immunol. 192 (2014) 2384–2394.
[33] L. Pan, B. Zhu, W. Hao, X. Zeng, S.A. Vlahopoulos, T.K. Hazra, M.L. Hegde, Z. Radak, A. Bacsi, A.R. Brasier, X. Ba, I. Boldogh, Oxidized guanine base lesions function in 8-Oxoguanine DNA Glycosylase-1-mediated epigenetic regulation of nuclear factor kappaB-driven gene expression, J. Biol. Chem. 291 (2016) 25553–25566.
[34] L. Pan, W. Hao, X. Zheng, X. Zeng, A. Ahmed Abbasi, I. Boldogh, X. Ba, OGG1-DNA interactions facilitate NF-kappaB binding to DNA targets, Sci. Rep. 7 (2017) 43297.
[35] L. Aguilera-Aguirre, A. Bacsi, A. Saavedra-Molina, A. Kurosky, S. Sur, I. Boldogh, Mitochondrial dysfunction increases allergic airway inflammation, J. Immunol. 183 (2009) 5379–5387.
[36] B. Tian, J. Yang, A.R. Brasier, Two-step cross-linking for analysis of protein-chromatin interactions, Methods Mol. Biol. 809 (2012) 105–120.
[37] Z. Chen, S.S. Viboolsittiseri, B.P. O'Connor, J.H. Wang, Target DNA sequence directly regulates the frequency of activation-induced deaminase-dependent mutations, J. Immunol. 189 (2012) 3970–3982.
[38] L. Feng, Y. Xia, G.E. Garcia, D. Hwang, C.B. Wilson, Involvement of reactive oxygen intermediates in cyclooxygenase-2 expression induced by interleukin-1, tumor necrosis factor-alpha, and lipopolysaccharide, J. Clin. Invest 95 (1995) 1669–1675.
[39] H. Thorvaldsdottir, J.T. Robinson, J.P. Mesirov, Integrative genomics viewer (IGV): high-performance genomics data visualization and exploration, Brief. Bioinform 14 (2013) 178–192.
[40] J.T. Robinson, H. Thorvaldsdottir, W. Winckler, M. Guttman, E.S. Lander, G. Getz, J.P. Mesirov, Integrative genomics viewer, Nat. Biotechnol. 29 (2011) 24–26.
[41] E. Eden, R. Navon, I. Steinfeld, D. Lipson, Z. Yakhini, GOrilla: a tool for discovery and visualization of enriched GO terms in ranked gene lists, BMC Bioinforma. 10 (2009) 48.
[42] J. Morreall, K. Limpose, C. Sheppard, Y.W. Kow, E. Werner, P.W. Doetsch, Inactivation of a common OGG1 variant by TNF-alpha in mammalian cells, DNA Repair (Amst.) 26 (2015) 15–22.
[43] S. Vlahopoulos, I. Boldogh, A. Casola, A.R. Brasier, Nuclear factor-kappaB-dependent induction of interleukin-8 gene expression by tumor necrosis factor alpha: evidence for an antioxidant sensitive activating pathway distinct from nuclear translocation, Blood 94 (1999) 1878–1889.
[44] M. Jamaluddin, S. Wang, I. Boldogh, B. Tian, A.R. Brasier, TNF-alpha-induced NF-kappaB/RelA Ser(276) phosphorylation and enhanceosome formation is mediated by an ROS-dependent PKAc pathway, Cell Signal 19 (2007) 1419–1433.
[45] A.R. Brasier, The NF-kappaB regulatory network, Cardiovasc Toxicol. 6 (2006) 111–130.
[46] G. Li, K. Yuan, C. Yan, J. Fox 3rd, M. Gaid, W. Breitwieser, A.K. Bansal, H. Zeng, H. Gao, M. Wu, 8-Oxoguanine-DNA glycosylase 1 deficiency modifies allergic airway inflammation by regulating STAT6 and IL-4 in cells and in mice, Free Radic. Biol. Med 52 (2012) 392–401.
[47] A. Gu, G. Ji, L. Yan, Y. Zhou, The 8-oxoguanine DNA glycosylase 1 (ogg1) decreases the vulnerability of the developing brain to DNA damage, DNA Repair (Amst.) 12 (2013) 1094–1104.
[48] L. Yan, Y. Zhou, S. Yu, G. Ji, L. Wang, W. Liu, A. Gu, 8-Oxoguanine DNA glycosylase 1 (ogg1) maintains the function of cardiac progenitor cells during heart formation in zebrafish, Exp. Cell Res 319 (2013) 2954–2963.
[49] P. German, D. Saenz, P. Szaniszlo, L. Aguilera-Aguirre, L. Pan, M.L. Hegde, A. Bacsi, G. Hajas, Z. Radak, X. Ba, S. Mitra, J. Papaconstantinou, I. Boldogh, 8-Oxoguanine DNA glycosylase1-driven DNA repair-A paradoxical role in lung aging, Mech. Ageing Dev. 161 (2017) 51–56.
[50] G. Ghosh, G. van Duyne, S. Ghosh, P.B. Sigler, Structure of NF-kappa B p50 homodimer bound to a kappa B site, Nature 373 (1995) 303–310.
[51] J. Yang, A. Mitra, N. Dojer, S. Fu, M. Rowicka, A.R. Brasier, A probabilistic approach to learn chromatin architecture and accurate inference of the NF-kappaB/RelA regulatory network using ChIP-Seq, Nucleic Acids Res 41 (2013) 7240–7259.
[52] L. Aguilera-Aguirre, A. Bacsi, Z. Radak, T.K. Hazra, S. Mitra, S. Sur, A.R. Brasier, X. Ba, I. Boldogh, Innate inflammation induced by the 8-oxoguanine DNA glycosylase-1-KRAS-NF-kappaB pathway, J. Immunol. 193 (2014) 4643–4653.
[53] L. Aguilera-Aguirre, K. Hosoki, A. Bacsi, Z. Radak, T.G. Wood, S.G. Widen, S. Sur, B.T. Ameredes, A. Saavedra-Molina, A.R. Brasier, X. Ba, I. Boldogh, Whole transcriptome analysis reveals an 8-oxoguanine DNA glycosylase-1-driven DNA repair-dependent gene expression linked to essential biological processes, Free Radic. Biol. Med 81 (2015) 107–118.
[54] F.E. Chen, D.B. Huang, Y.Q. Chen, G. Ghosh, Crystal structure of p50/p65 heterodimer of transcription factor NF-kappaB bound to DNA, Nature 391 (1998) 410–413.
[55] S.S. Wallace, DNA glycosylases search for and remove oxidized DNA bases, Environ. Mol. Mutagen 54 (2013) 691–704.
[56] H.S. Kim, B.H. Kim, J.E. Jung, C.S. Lee, H.G. Lee, J.W. Lee, K.H. Lee, H.J. You, M.H. Chung, S.K. Ye, Potential role of 8-oxoguanine DNA glycosylase 1 as a STAT1 coactivator in endotoxin-induced inflammatory response, Free Radic. Biol. Med 93 (2016) 12–22.
[57] A. Sassa, W.A. Beard, R. Prasad, S.H. Wilson, DNA sequence context effects on the glycosylase activity of human 8-oxoguanine DNA glycosylase, J. Biol. Chem. 287 (2014) 36702–36710.
[58] J.W. Hill, T.K. Hazra, T. Izumi, S. Mitra, Stimulation of human 8-oxoguanine-DNA glycosylase by AP-endonuclease: potential coordination of the initial steps in base excision repair, Nucleic Acids Res 29 (2001) 430–438.
[59] A. Bravard, M. Vacher, B. Gouget, A. Coutant, F.H. de Boisferon, S. Marsin, S. Chevillard, J.P. Radicella, Redox regulation of human OGG1 activity in response to cellular oxidative stress, Mol. Cell Biol. 26 (2006) 7430–7436.

[60] M. Wu, H. Huang, W. Zhang, S. Kannan, A. Weaver, M. McKibben, D. Herington, H. Zeng, H. Gao, Host DNA repair proteins in response to Pseudomonas aeruginosa in lung epithelial cells and in mice, Infect. Immun. 79 (2011) 75–87.
[61] S.D. Bruner, D.P. Norman, G.L. Verdine, Structural basis for recognition and repair of the endogenous mutagen 8- oxoguanine in DNA, Nature 403 (2000) 859–866.
[62] J.T. Stivers, Site-specific DNA damage recognition by enzyme-induced base flipping, Prog. Nucleic Acid. Res Mol. Biol. 77 (2004) 37–65.
[63] S.S. Wallace, Biological consequences of free radical-damaged DNA bases, Free Radic. Biol. Med 33 (2002) 1–14.
[64] A. Chakraborty, M. Wakamiya, T. Venkova-Canova, R.K. Pandita, L. Aguilera-Aguirre, A.H. Sarker, D.K. Singh, K. Hosoki, T.G. Wood, G. Sharma, V. Cardenas, P.S. Sarkar, S. Sur, T.K. Pandita, I. Boldogh, T.K. Hazra, Neil2-null mice accumulate oxidized DNA bases in the transcriptionally active sequences of the genome and are susceptible to innate inflammation, J. Biol. Chem. 290 (2015) 24636–24648.
[65] X. Ba, I. Boldogh, 8-Oxoguanine DNA glycosylase 1: beyond repair of the oxidatively modified base lesions, Redox Biol. 14 (2018) 669–678.
[66] L. Xia, W. Huang, M. Bellani, M.M. Seidman, K. Wu, D. Fan, Y. Nie, Y. Cai, Y.W. Zhang, L.R. Yu, H. Li, C.A. Zahnow, W. Xie, R.W. Chiu Yen, F.V. Rassool, S.B. Baylin, CHD4 has oncogenic functions in initiating and maintaining epigenetic suppression of multiple tumor suppressor genes (e657), Cancer Cell 31 (2017) 653–668 (e657).
[67] X. Zhou, W. Wang, C. Du, F. Yana, S. Yang, K. He, H. Wang, OGG1 regulates the level of symmetric dimethylation of histone H4 arginine-3 by interacting with PRMT5, Mol. Cell. Probes 38 (2018) 19–24.